Numerical modeling of windblown dust in the Pacific Northwest with improved meteorology and dust emission models

Irra Sundram, Candis Claiborn, Tara Strand, and Brian Lamb

Laboratory for Atmospheric Research, Department of Civil and Environmental Engineering, Washington State University, Pullman, Washington, USA

Dave Chandler

Department of Plants, Soils and Biometeorology, Utah State University, Logan, Utah, USA

Keith Saxton

U.S. Department of Agriculture Agricultural Research Service, Washington State University, Pullman, Washington, USA

Received 19 March 2004; revised 27 September 2004; accepted 18 October 2004; published 21 December 2004.

[1] Soil erosion by wind is a serious consequence of dry land agriculture in eastern Washington, where the main adverse effects are loss of nutrient-rich soil, reduced visibility during dust storms and degradation of air quality. A multidisciplinary research effort to study windblown dust in central and eastern Washington was initiated under the Columbia Plateau PM_{10} (CP_3) program, which involved measuring wind erosion and windblown dust emissions at sites throughout the region and developing a transport and dispersion model for the area. The modeling system includes the prognostic meteorological model, Mesoscale Metorological Model Version 5 (MM5), coupled with the CALMET/CALGRID Eularian modeling pair and a new dust emission module (EMIT-PM). Improvements to the modeling system included employing higher spatial resolutions for the meteorological models and improved parameterizations of emission factors in EMIT-PM. Meteorological fields, dust emissions and the resulting dust concentrations were simulated for six historical regional dust storms: 23 November 1990, 21 October 1991, 11 September 1993, 3 November 1993, 30 August 1996 and 23–25 September 1999. For all the simulated events, with the exception of the August 1996 event, ratios of observed to predicted concentrations were favorable, within a range of 0.5–6.0 without calibration of the dust emission model; PM_{10} emissions averaged 22 Gg per 24-hour event, representing approximately 1% of the daily dust flux on a global basis. These results showed that the model performed best for large, strong dust storms but did not simulate smaller storms as well. *INDEX TERMS:* 0305 Atmospheric Composition and Structure: Aerosols and particles (0345, 4801); 0345 Atmospheric Composition and Structure: Pollution—urban and regional (0305); 4801 Oceanography: Biological and Chemical: Aerosols (0305); 4805 Oceanography: Biological and Chemical: Biogeochemical cycles (1615); *KEYWORDS:* dust storm, numerical simulation, wind erosion

Citation: Sundram, I., C. Claiborn, T. Strand, B. Lamb, D. Chandler, and K. Saxton (2004), Numerical modeling of windblown dust in the Pacific Northwest with improved meteorology and dust emission models, *J. Geophys. Res.*, *109*, D24208, doi:10.1029/2004JD004794.

1. Introduction

[2] Soil erosion by wind is a serious consequence of dry land agriculture in many parts of the world. This is especially pervasive in the Pacific Northwest, where because of low precipitation rates of 150 to 360 mm/yr, dry land farming involves alternate years of cropping and clean tilled fallow land. During the fallow years, the soil is periodically tilled for weed control and this results in loosely structured clods on bare surfaces, which are very susceptible to wind erosion [*Horning et al.*, 1998]. The amount of soil loss from erosion is dependent on the local meteorology and soil morphology, and losses ranging from 0.3 to 30.4 Mg ha^{-1} per erosion event have been reported from monitoring studies in Alberta, Canada [*Larney et al.*, 1995]. An erosion monitoring study in Texas conducted over 18 months, indicated that most erosion events are associated with periods of low humidity (<30%), low precipitation, no surface cover and daily wind speeds greater than 4 m s^{-1}, and similar conditions have also been associated with erosion events in the Pacific Northwest [*Stout*, 2001].

[3] The main adverse effects of soil erosion on agriculture in the Pacific Northwest are decline in soil quality due to removal of nutrient rich aggregates, reduced soil productiv-

0148-0227/04/2004JD004794$09.00

ity and subsequently, reduced crop yield. Windblown dust also leads to air quality and public health issues as finer fractions (<10 μm) of the entrained dust are transported downwind of the source regions. However, declining visibility is usually of immediate concern during a dust storm episode. For example, visibility in the Korean peninsula decreased from 60 km to 2 km as the hourly PM_{10} concentrations increased from 32 to 600 μg m^{-3} during the Chinese Yellow Sand event in 2000 [*Kim et al.*, 2001]. In the Pacific Northwest, poor visibility during a dust storm event in 1999 resulted in a 50-car pile-up and seven deaths on Interstate 84 near Hermiston, Oregon. These adverse effects coupled with violations of the National Ambient Air Quality Standards for PM_{10} in several urban areas in eastern Washington motivated the formation and long-term support of the Columbia Plateau PM_{10} Program http://pnw-winderosion.wsu.edu).

[4] In recent years, there has been considerable debate on the climate forcing potential of atmospheric dust, with current global emissions estimated to range between 1000 and 5000 Tg yr^{-1} [*Xuan and Sokolik*, 2002; *Ginoux et al.*, 2001; *Houser and Nickling*, 2001]. Since 30 to 50% of the dust load is predicted to originate from soil disturbed by human activities, determination of this forcing potential should consider climate-anthropogenic activities feedback cycles [*Tegen and Fung*, 1995]. However, sparse information on the microphysical, chemical and optical properties of atmospheric dust contribute toward the unresolved and poorly understood issue of the influence of atmospheric dust on local climatology and on global and regional radiative budgets [*Tegen*, 2003; *Yu et al.*, 2001].

[5] Modeling mobilization of dust from soils is usually described in terms of creep, saltation and resuspension of soil, based on the assumption that vertical dust flux is a function of the surface shear stress [*Houser and Nickling*, 2001; *Tegen and Fung*, 1994; *Fryrear et al.*, 1991]. This assumption is often applied in terms of a power law relationship between the vertical flux of dust and friction velocity: $F = Cu_*^n$, where C is a calibrated, empirical constant. In their global simulation of the atmospheric dust cycle, *Tegen and Fung* [1994] adjusted C to obtain agreement between predicted and estimated source strengths; the range of C was between 0.4 and 1.2 μg s^2 m^{-5} in the relationship $F = C\,(u - u_t)^n$, where u_t is a threshold wind speed that must be exceeded in order to produce windblown dust. *Ginoux et al.* [2001] improved dust source characterizations in the GOCART model and were able to reproduce seasonal variations of global surface concentrations using a C value of 1 μg s^2 m^{-5}.

[6] On a regional scale, mobilization of soil from eroding surfaces has been further parameterized in terms of physical soil properties such as mechanical stability of clods, aggregates, crust, surface cover and roughness conditions [*Draxler et al.*, 2001; *Horning et al.*, 1998]. To develop their dust production model (DPM), *Alfaro and Gomes* [2001] combined empirical based models describing saltation and sandblasting and successfully validated the DPM with field measurements for PM_{20} emissions from various soil types in Spain and Niger [*Gomes et al.*, 2003]. *Draxler et al.* [2001] parameterized vertical mass flux for PM_{10} for sandy desert soil using friction velocity, threshold friction velocity and a parameter defining surface soil textures. In eastern Washington, a dust model (EMIT) based on abrasion and suspension processes was developed for PM_{10} emissions through independent experiments characterizing the effect of emission variables (e.g., roughness elements, surface crusting) on total emissions for specific soil types and farming practices. Statistical analyses were then employed to develop relationships between horizontal soil flux and PM_{10} emissions [*Saxton et al.*, 2000; *Horning et al.*, 1998; *Saxton*, 1995].

[7] For validation, *Claiborn et al.* [1998] employed EMIT with the CALMET/CALGRID models to simulate two dust storms in eastern Washington and found that C values of 9.6×10^{-3} and 1.5×10^{-3} g s^3 m^6 were required to achieve ratios of observed to predicted PM_{10} concentrations of 0.5 to 3.6. Variations in C in that study reflected changes in soil parameters, especially moisture content, over the fall season. On the basis of the recommendations from *Claiborn et al.* [1998], efforts to improve the dust emission algorithm were carried out by *Saxton et al.* [2000]. This resulted in a modified emissions model (EMIT-PM), developed specifically for the Pacific Northwest from extensive soil sampling, portable wind tunnel and intensive field measurements. *Lee* [1998] utilized the revised code to model five dust storm events, which occurred in the Pacific Northwest, but C still required calibration to match predictions to available observations. In the study by *Lee* [1998], the values for C accounted for the overall effects of remaining uncertainties in the emissions model and exhibited large fluctuations for the different events. Subsequently, *Chandler et al.* [2002] incorporated better estimates of the suspendable soil fraction (PM_{10}), described by the soil dustiness index in the emission algorithm, in a revised version of the EMIT-PM.

[8] The intent of this study was to evaluate the improvements in EMIT-PM as part of a high-resolution regional windblown dust model to predict PM_{10} emissions, transport and dispersion for large regional dust storms in the Pacific Northwest. This modeling effort has important regulatory implications since several populated areas in eastern Washington (e.g., Spokane) have been designated as ''nonattainment'' areas for PM_{10} concentrations in the past, and therefore appropriate erosion mitigation strategies are required to control urban air quality impact from agricultural wind erosion [*Saxton*, 1995]. Development of this regional modeling system also provides a foundation for investigation of the effectiveness of wind erosion control strategies (e.g., increase in vegetative surface cover) in reducing PM_{10} concentrations in downwind populated areas and the impact of intense regional dust storms upon aerosol optical depth and in turn, global climate change.

[9] Utilization of the revised EMIT-PM in conjunction with MM5, CALMET and CALGRID in this study provided an opportunity to identify dust sources and quantify PM_{10} emissions from agricultural regions and predict hourly variations of PM_{10} concentrations in populated areas during six historical dust storm events in eastern Washington. To test emission algorithms in EMIT-PM, the calibrated dust constant, C, was not invoked. An overview of the modeling system, including descriptions of the modeling components and the empirically derived emissions parameters, is presented in section 2 and before results from the simulations of six individual case studies are discussed in section 3.

Table 1. Estimated Values for Surface Cover, Surface Roughness, Water Content, and Aerodynamic Roughness in the EMIT-PM Model for Major Land Use Categories and Events[a]

Event	Parameters	Land Use Categories				
		RL	IRR	DC	DF	CRP
23 November 1990	SC	70	10	90	15	70
	K	1.8	1.3	1.8	1.3	1.8
	WC	0.1	0.8	0.1	0.5	0.1
	Zo	4	1	5	0.6	4
21 October 1991	SC	70	25	90	10	70
	K	1.8	1.3	1.8	1.8	1.8
	WC	0.1	0.9	0.3	0.9	0.1
	Zo	4	1	5	0.6	4
11 September 1993	SC	70	50	90	5	70
	K	1.8	1.3	1.8	2	1.8
	WC	0.1	0.8	0.1	1	0.1
	Zo	4	1	1	0.6	4
3 November 1993	SC	70	20	90	10	70
	K	1.8	1.3	1.8	1.8	1.8
	WC	0.1	0.9	0.2	0.8	0.1
	Zo	4	1	5	0.6	4
30 August 1996	SC	70	20	90	5	70
	K	1.8	1.3	1.8	1.3	1.8
	WC	0.1	1	0.1	1	0.1
	Zo	4	1	5	0.3	4
23–25 September 1999	SC	70	50	90	5	70
	K	1.8	1.3	1.8	2	1.8
	WC	0.1	0.8	0.1	1	0.1
	Zo	4	1	1	0.6	4

[a]SC, surface cover (percent); K, surface roughness (cm), WC, water content (dimensionless), and z_o, aerodynamic roughness (cm). Land use categories are rangeland (RL), irrigated (IRR), dry crop (DC), dry fallow (DF), and conservation resource program (CRP).

Statistical performances of various components of the model are also discussed.

2. Overview of the Modeling System

2.1. EMIT-PM Emissions Model

[10] EMIT-PM was developed to determine the fraction of dust emissions contributing from eroding fields that contribute toward PM_{10} regional concentrations. The model is based upon two semi-empirical equations describing horizontal and vertical soil fluxes. The horizontal soil flux as described by *Saxton et al.* [2000] is a function of the available wind energy, soil erodibility, vegetative surface cover, soil surface roughness, soil surface wetting and crusting. On the basis of extensive wind tunnel and field measurements, these variables can be described empirically in the horizontal soil flux equation

$$Q_t = W_t * EI * \left(e^{-0.05 * SC} * e^{-0.52 * K}\right) * WC, \quad (1)$$

where Q_t is the eroded soil discharge per meter field width per unit time, (g m^{-1} width per hour event) and W_t is the erosive wind energy per unit time (m^3 s^{-3} per hour event). The wind energy term includes a threshold wind speed (U_{te}) required to initiate soil movement on the ground. On the basis of extensive field characterizations during dust events on the Columbia Plateau, U_{te} was defined as 5.5 m s^{-1} for all events modeled in this study. EI describes the erodibility potential of unprotected soil (g s^3 m^{-3}) and is calculated from the relative erodibility ratio (ER) obtained from wind tunnel trials for each soil type. SC is the percentage of vegetative soil cover and K describes the random roughness of large soil elements (cm). WC is a nondimensional index from 0 to 1 describing the degree of wetness and crusting of the soil. Wet, crusted soil has less potential for erosion and is represented by a lower WC value as opposed to higher values associated with dry, disturbed, noncrusted soil [*Saxton et al.*, 2000].

[11] The vertical flux of PM_{10} (g m^{-2} s^{-1}) is described as a function of the horizontal soil flux, soil dustiness, wind velocity and the calibrated nondimensional dust constant, C(= 1 in this study), in the following form:

$$F_d = C * C_v * u_* * Q_t * (D/100). \quad (2)$$

C_v is a unit conversion factor, u_* is the friction velocity (m s^{-1}), and D is the soil dustiness index. D was determined by a laboratory procedure utilizing soil samples, which were suspended and abraded in an emission cone prior to measurement of the PM_{10} fraction with a standard measuring instrument [*Chandler et al.*, 2002; *Saxton et al.*, 2000]. D was calculated as the ratio of the mass of suspended PM_{10} collected by the measuring instrument to the mass of suspended soil in the cone. The fraction of suspended PM_{10} as determined by *Chandler et al.* [2002] from suspension and abrasion processes was 3–6 times higher than previous measurements from *Saxton et al.* [2000], who only considered suspension mechanisms to compute D. Hence the D values utilized in this study were larger than the values utilized by *Lee* [1998] and *Claiborn et al.* [1998] and resulted in significantly larger PM_{10} emissions.

[12] Tables 1 and 2 summarize the input variables required for EMIT-PM as functions of landuse categories. SC, K, WC and Zo (aerodynamic roughness, cm) represent regional averages for various landuse categories in the model domain. SC, K and Zo were obtained through wind tunnel trials on 68 field plots and K through visual comparisons of test plots with well documented photographs from other studies [*Saxton et al.*, 2000]. The landuse categories are rangeland (RL), irrigated (IRR), dry crop (DC), dry fallow (DF), and conservation resource program (CRP). In Table 2, values for D reflect improved results from *Chandler et al.* [2002]. D and ER are functions of soil types common to Washington, Oregon and Idaho. L1 is the most erodible soil, L5

Table 2. Average Soil Dustiness and Relative Erodibility Ratio for the Major Soil Classes in the Columbia Plateau Region[a]

Soil Class	D Average	ER Average
DQ	0.50	6.660
DE	0.15	0.250
DS	2.66	0.239
L1A	1.98	1.000
L2A	2.94	0.550
L1B	3.39	0.480
L2B	3.05	0.320
L3	3.39	0.360
L4	4.38	0.420
L5	5.47	0.140

[a]D, soil dustiness (dimensionless); ER, relative erodibility ratio (dimensionless).

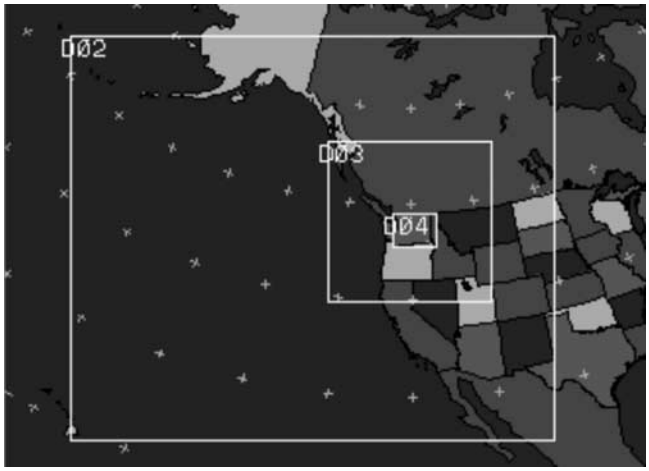

Figure 1. MM5 modeling domain, with nested grids of 36 km, 12 km and 4 km. See color version of this figure in the HTML.

is the least erodible soil whereas the D class soils are equal to L1 in terms of erosivity [*Lee*, 1998].

2.2. Meteorological Model MM5, MCIP2, and CALMET

[13] MM5 is a mesoscale meteorological model developed in the early 1970s and currently maintained as a community model by the National Center for Atmospheric Research. MM5 is a prognostic model capable of multiple domain nesting, nonhydrostatic dynamics, four-dimensional data assimilation (FDDA) and a variety of physics options, which allow for representative simulations of the meteorology in the domain of interest [*Dudhia et al.*, 2001]. In this study, MM5 was run in the nonhydrostatic mode to generate the wind fields for all six dust storm events. This application of MM5 for our regional dust modeling is an improvement over previous work by *Claiborn et al.* [1998] and *Lee* [1998] since those studies did not use a consistent meteorological modeling method for each dust event, and the horizontal grid scale resolution in the parent MM5 simulations were at a coarse scale in most cases.

[14] The horizontal winds from MM5 were utilized as the initial guess field in the diagnostic meteorological model, CALMET. The nested grids in MM5 had horizontal dimensions of 36, 12 and 4 km (Figure 1). The innermost domain (4 km) had 124 $\times$ 97 grids (longitude by latitude), which encompassed the state of Washington, northern Oregon and Idaho and southwestern Canada. FDDA, which incorporates analysis nudging, was applied to the 36 and 12 km domains. With this option, user-defined relaxation terms are applied to the prognostic equations and this serves to relax the model values toward an analysis obtained for the assimilation period [*Dudhia et al.*, 2001]. The analysis nudging coefficients for wind and temperature fields for the 36 km domain was 2.5×10^{-4} and 1.0×10^{-4} for the 12 km domain. One way nesting was used for interpolation from the 36 to 12 km domain and two way nesting was employed from the 12 km to the 4 km domain. In the vertical dimension, a terrain following coordinate system was utilized with 37 sigma layers.

[15] CALMET was utilized to develop mass consistent, three-dimensional wind fields for each event with interpolation of the MM5 winds with available surface wind observations. The innermost 4 km domain from MM5 was reduced to 88 $\times$ 76 grids (longitude by latitude), which encompassed an area from 45.425°N to 48.479°N and 121.000°E to 116.105°E (Figure 2). Figure 2 also displays the terrain elevation for this region, where the more mountainous regions corresponding to the Cascade mountain range are to the west and the flatter plains of the Columbia Plateau to the east, with an average elevation of approximately 800 m.

[16] To produce the final wind fields, observational data were introduced through an objective analysis procedure involving an inverse-distance squared interpolation scheme. This scheme allows for the utilization of observational data in the vicinity of the surface stations and the first step wind fields in regions of sparse or no observational data [*Elbir*, 2003]. The meteorological stations are mostly located in eastern Washington and surface data were available from 28 to 75 stations whereas upper air soundings were available from 1 to 4 stations among the six events. The required hourly observational data are wind speed, wind direction, temperature, cloud cover, ceiling cloud height, surface pressure and relative humidity [*Scire et al.*, 1999].

[17] The vertical layers were also reduced to 13 layers with the layer faces defined at 20, 36, 70, 110, 145, 215, 290, 400, 506, 656, 1000, 1695 and 3340 m above ground level. These layer heights were chosen to be compatible with the application of the MM5 postprocessor; Meteorology-Chemistry Interface Processor (MCIP2). MCIP2 is part of the USEPA's CMAQ modeling system and in this study, was employed to pass MM5 boundary layer terms, including mixed layer height, directly to CALGRID. In this way, the MM5 horizontal winds were interpolated with observations in CALMET, while all other boundary layer terms were obtained directly from MM5 via MCIP.

2.3. Transport and Dispersion Model CALGRID

[18] CALGRID solves the K-theory form of the atmospheric diffusion equation to obtain hourly averaged values of PM_{10} in each grid cell. In this case, PM_{10} particles are treated as inert tracers. The final transport and diffusion

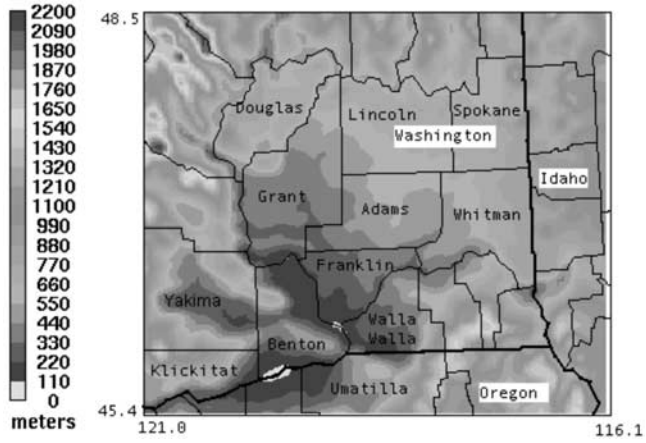

Figure 2. CALMET model domain and terrain elevation. See color version of this figure in the HTML.

Table 3. Location of Surface Stations and Summary of Available PM_{10} Measurements for Each Event

Stations	Location and Description			Dust Storm Events
	Latitude, °N	Longitude, °W	Description	
Crown Zellerbach (CZ)	47.66	117.36	industrial, Spokane	21 Oct. 1991; 11 Sept. 1993; 3 Nov.1993; 30 Aug. 1996; 23–25 Sept. 1999
Rockwood (RW)	47.75	117.41	residential, Spokane	23 Nov. 1990, 21 Oct.1991; 11 Sept. 1993; 3 Nov. 1993; 30 August 1996
Millwood (MW)	47.69	117.28	light commercial, Spokane	21 Oct. 1991; 3 Nov. 1993
Spokane Auto Glass (SAG)	47.63	117.53	urban, Spokane	11 Sept. 1993; 3 Nov. 1993
Turnbull (TB)	47.36	117.61	wildlife refuge, SW of Spokane	11 Sept. 1993
Kennewick (KW)	46.21	119.14	urban, Kennewick	23 Nov. 1990; 21 Oct. 1991; 11 Sept. 1993; 3 Nov. 1993; 23–25 Sept. 1999

equation solved for each time step in each grid cell can be represented by

$$\frac{\partial \bar{c}}{\partial t}+\frac{\partial \overline{uc}}{\partial x}+\frac{\partial \overline{vc}}{\partial y}+\frac{\partial \overline{wc}}{\partial z}-\frac{\partial}{\partial x}\left(Kx\frac{\partial \bar{c}}{\partial x}\right)-\frac{\partial}{\partial y}\left(Ky\frac{\partial \bar{c}}{\partial y}\right)-\frac{\partial}{\partial z}\left(Kz\frac{\partial \bar{c}}{\partial z}\right)=R+S+L \quad (3)$$

where K represents the eddy diffusivity tensor and R represents photochemical processes, which were not utilized in this study, S represents emission sources and L represents losses from deposition processes [*Yamartino et al.*, 1992]. CALGRID employs a higher-order chapeau scheme to solve the advection terms. The model employs the Smargorinsky method to compute diffusivities due to distortion or stress in the horizontal wind field. Vertical diffusivities (Kz) are estimated using convective scaling in the daytime boundary layer and local scaling in the nighttime boundary layer [*Scire et al.*, 1989]. The hourly emissions from erodible soil in the target domain (i.e., the S term in the transport and diffusion equation) were provided by EMIT-PM. The horizontal grid system of 88 grids × 76 grids and 13 vertical layers employed in CALMET were maintained for the CALGRID simulations as well. The dry deposition velocity was specified as a constant at 0.1 cm s^{-1}.

2.4. Description of PM_{10} Episodes and Surface Observations

[19] Surface measurements of ambient PM_{10} at various receptor sites are available for all six dust storm events and were used to evaluate model predictions. These measurements are gravimetrically determined hourly (TEOM) or averaged 24-hour PM_{10} concentrations, measured by the Spokane and Benton County Air Pollution Control Authorities located in Spokane and Kennewick, Washington (see Table 3 and Figure 2). Background concentrations of PM_{10} tend to vary between 30 and 80 μg m^{-3} from rural to urban sites, respectively [*Claiborn et al.*, 1998].

[20] Six dust storm events were simulated and analyzed: 23 November 1990, 21 October 1991, 11 September 1993, 3 November 1993, 30 August 1996, and 23–25 September 1999. These events occurred mainly because of strong southwesterly winds associated with low-pressure systems, which resulted in wind speeds exceeding 6.0 m s^{-1} with gusts up to 15 m s^{-1} and violations of the NAAQS standards at one or more of the sampling stations over the source locations and urban areas. *Claiborn et al.* [1998] analyzed a number of dust storms and identified a characteristic weather pattern associated with these regional dust storms that involved an intense surface low-pressure system moving quickly across southern Canada coupled with a high-pressure system centered over Nevada. In all these events, as the synoptic system weakened, declining wind speeds resulted in cessation of blowing dust in the region. Locations with available average 24-hour PM_{10} concentrations for each event are summarized in Table 3. For the 1993 and 1999 events, hourly averaged PM_{10} concentrations from monitors are presented.

3. Results and Discussion

[21] Predicted PM_{10} concentrations and comparison with measurements for each event are presented in this section. Ideally, predictions should be evaluated with continuous measurements from a dense network of sampling stations to fully resolve spatial heterogeneities and temporal patterns of the dust plume. However, PM_{10} measurements are relatively scarce for this region, and only a limited number of measurements were available during each event in this study; hence subgrid spatial and temporal heterogeneities not simulated by the model may contribute to uncertainties in comparing model results to just a few observation points.

[22] Emission fluxes and PM_{10} mass concentrations are discussed in units of kg km^{-2} hr^{-1} and mg m^{-3}, respectively. Units of g km^{-2} hr^{-1} and μg m^{-3} are utilized for low emission fluxes and PM_{10} concentrations. Unless explicitly stated, discussions are in Pacific Standard Time (PST).

3.1. Events of 23 November 1990 and 21 October 1991

[23] On 23 November 1990 the prevailing winds were southwesterly and in Kennewick (KW), wind speeds exceeded 9.0 m s^{-1} throughout the morning. In Yakima County, predicted maximum average 24-hour PM_{10} concentration was 6.7 mg m^{-3} (Figure 3). In KW and Rockwood (RW), observed average 24-hour PM_{10} concentrations were 251 and 126 μg m^{-3}, respectively and while these concentrations were overpredicted with observed to predicted concentrations ratios of 0.53 in KW and 0.76 in RW (Table 4), the overall magnitude of the event was reasonably well predicted.

[24] For the 21 October 1991 event, maximum wind speeds in Spokane were 19.5 m s^{-1} in southerly to southwesterly flow. Figure 4 presents the predicted average 24-hour PM_{10} concentrations with a maximum concentration of 0.6 mg m^{-3} in Lincoln County. This event was underpredicted at Crown Zellerbach (CZ), Millwood (MW), RW and KW with observed to predicted concen-

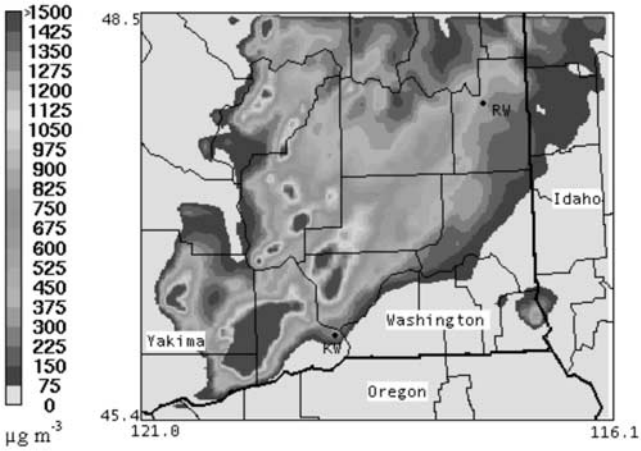

Figure 3. Predicted average 24-hour PM_{10} concentrations, 23 November 1990. See color version of this figure in the HTML.

trations ratios ranging from 6 to 12 (Table 4). In general, this underestimation could be due to errors associated with predicting the meteorology and emissions in the source regions.

3.2. Events of 11 September and 3 November 1993

[25] On 11 September a low-pressure system was centered over Canada, resulting in strong southwesterly surface winds in the Pacific Northwest with concentrations exceeding 2000 μg m^{-3} in Spokane [*Claiborn et al.*, 1998].

Table 4. Summary of Observed and Predicted 24-Hour PM_{10} Average Concentrations

Location	Observed PM_{10}, μg m^{-3}	Predicted PM_{10}, μg m^{-3}	Observed/Predicted
	23 November 1990		
RW	251	332	0.76
KW	126	237	0.53
	21 October 1991		
CZ	361	62	5.8
MW	305	59	5.2
RW	267	90	3.0
KW	1035	89	11.6
	11 September 1993		
CZ	300	73.0	4.1
SAG	297	74.5	4.0
RW	255	54.0	4.6
TB	490	106.0	4.6
KW	118	103.0	1.1
	3 November 1993		
CZ	207	82	2.5
SAG	156	95	1.6
MW	176	59	3.0
RW	100	96	1.0
	30 August 1996		
RW	212	1.2	175
CZ	128	0.95	135
	23–25 September 1999		
CZ	400	155	2.58
KW	630	808	0.78

Maximum PM_{10} emissions were 5 kg km^{-2} s^{-1}, predicted to occur in Grant and Douglas Counties and this resulted in a maximum average 24-hour PM_{10} concentration of 6.9 mg m^{-3} in Douglas County (Figure 5). This result differs from *Claiborn et al.* [1998], who identified KW and the surrounding areas as the dust source for this event. It is expected that the results in the current study would be more accurate because of the improvements by *Chandler et al.* [2002] to D in EMIT-PM. In general, however, PM_{10} concentrations were underpredicted at all the sampling locations (Table 4).

[26] Predicted hourly concentrations were evaluated against hourly averaged PM_{10} concentrations measured with a Tapered Element Oscillating Microbalance (TEOM). The error bars in Figure 6 reflect the standard deviation obtained from averaging the concentrations in nine 4 km by 4 km grid cells surrounding the location of the sampling station. Elevated PM_{10} concentrations in Figure 6 were observed from 0500 PST and the peak at 1600 PST coincided with maximum wind speeds of 12 m s^{-1}. The maximum PM_{10} concentration of 0.5 mg m^{-3} was under predicted and displaced temporally but the relative magnitudes of the maximum and minimum concentrations were well simulated.

[27] In the 3 November 1999 event, PM_{10} emissions were predicted to exceed 2000 kg km^{-2} s^{-1} in Klickitat County and advection from the source region resulted in maximum PM_{10} concentrations of 8.5 mg m^{-3} in Umatilla County (Oregon) (Figure 7). Observed to predicted average 24-hour PM_{10} concentration ratios at the sampling stations indicate excellent agreement (1.0 to 2.5; Table 4). Figure 8 shows a comparison of the hourly averaged observed and predicted concentrations at RW. Wind speeds at RW remained elevated above 8.0 m s^{-1} until 1300, which matches the patterns in the observed PM_{10} concentration peaks. Even though the maximum PM_{10} concentration appears to be displaced temporally by approximately 6 hours, as with the 11 September 1993 event, the relative magnitudes of maximum and minimum PM_{10} concentrations are well represented.

3.3. Event of 30 August 1996

[28] This event was unique as it occurred in the summer season. The source region was identified in Douglas County,

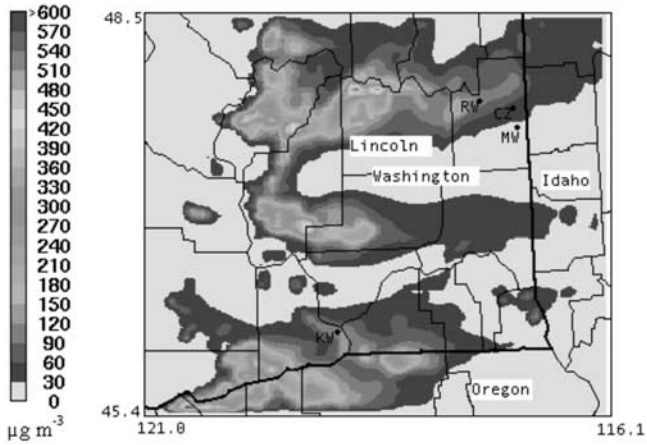

Figure 4. Predicted average 24-hour PM_{10} concentrations, 21 October 1991. See color version of this figure in the HTML.

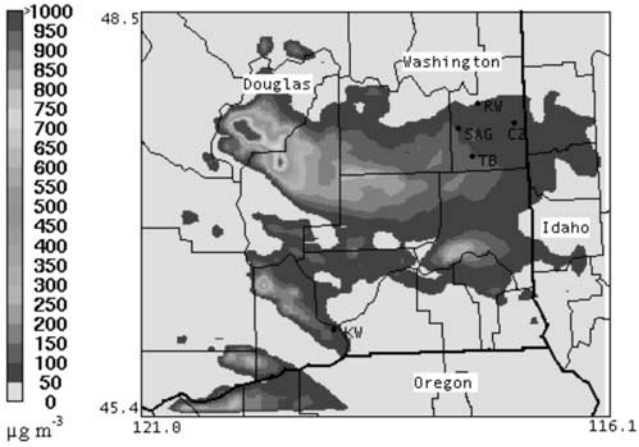

Figure 5. Predicted average 24-hour PM_{10} concentrations, 11 September 1993. See color version of this figure in the HTML.

with maximum PM_{10} emissions of 7.4 mg m^{-3} (Figure 9). Predicted average 24-hour PM_{10} concentrations at RW and CZ were 1.2 and 0.95 µg m^{-3}, vastly underpredicted from the observed concentrations of 212 and 128 µg m^{-3} at RW and CZ, respectively (Table 4). This was the smallest event simulated in terms of strength of wind and duration of the storm. Further analysis of the simulation problems with this event is discussed in section 4.

3.4. Events of 23–25 September 1999

[29] The large dust storm events of September 1999 occurred over a 3-day period with PM_{10} concentrations near source regions in Umatilla County predicted to be 6.3 mg m^{-3} on 23 September and 0.5 mg m^{-3} on 25 September. Predicted and observed hourly concentrations at KW and CZ are presented in Figures 10 and 11, respectively. In general, simulations captured the onset of the dust event in Kennewick (Figure 10), which occurred on 25 September but failed to predict the observed peak concentrations of 1.7 mg m^{-3} at 1200 PST on 23 September. The maximum predicted concentration for this 3-day event was 3.0 mg m^{-3} on 24 September at 2300 PST, predicted to occur 2 hours ahead of the observed maximum for that period, which was 1.7 mg m^{-3} at 0100 PST, 25 September. Comparisons made against observations during periods when observed concentrations exceeded 80 µg m^{-3} (Table 4) resulted in a reasonable observed to predicted ratio of 0.78.

[30] In Spokane (Figure 11), the model predicted the onset of elevated PM_{10} concentrations on 23 September, even though the predicted maximum concentration of 0.1 mg m^{-3} at 1900 PST is an underestimation of the observed maximum concentration of 0.4 mg m^{-3}, which occurred 3 hours later at 2200 PST. On 25 September, observed maximum PM_{10} concentration of 1.5 mg m^{-3} occurred at 1000 PST corresponding to maximum wind speeds of 15.4 m s^{-1}, whereas the predicted maximum was 0.7 mg m^{-3} at 0500 PST. The statistical comparison of model predictions to observed concentrations for Spokane are presented in Table 4. For Spokane, the model underestimated PM_{10} concentrations by a factor of almost 2.6, even though the overall distribution trend was fairly well represented. The model also failed to predict the magnitude of the maximum observed concentration and the timing of its occurrence. However, it is encouraging to note that the observed to predicted PM_{10} concentration ratios for both KW and Spokane are well within the overall range of values obtained for the previous events, with the exception of the 30 August 1996 event.

4. Summary of Model Performance

[31] Table 5 is a summary of the statistics detailing the performance of the modeling system against observed meteorological observations for each event. To compute the statistics, 20 surface stations, representing urban and rural areas, were chosen for each event, except for the September 1999 event, for which only 9 surface stations were available. These measurements are hourly averages from a network of meteorological stations and were incorporated into CALMET to improve model predictions, and therefore these tests are not independent verifications of the model performance. However, they are valuable tools to utilize as an overall representation and analyses of the wind speeds and wind directions.

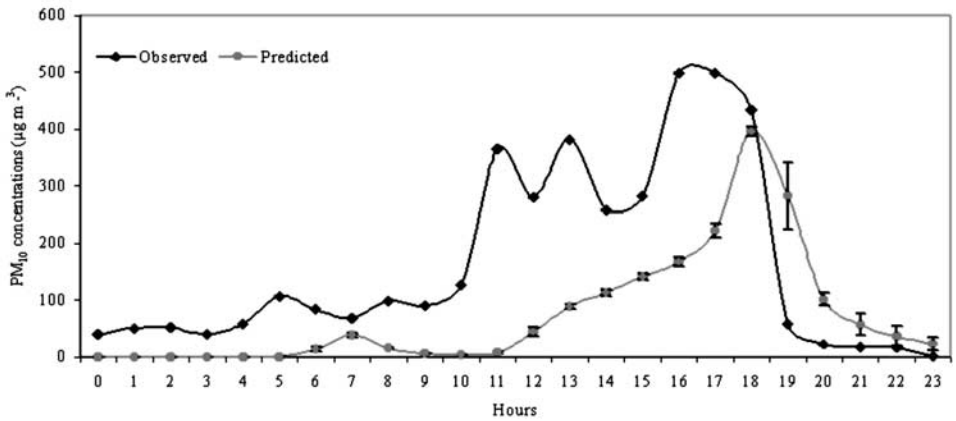

Figure 6. Predicted and measured PM_{10} concentrations at CZ, 11 September 1993. See color version of this figure in the HTML.

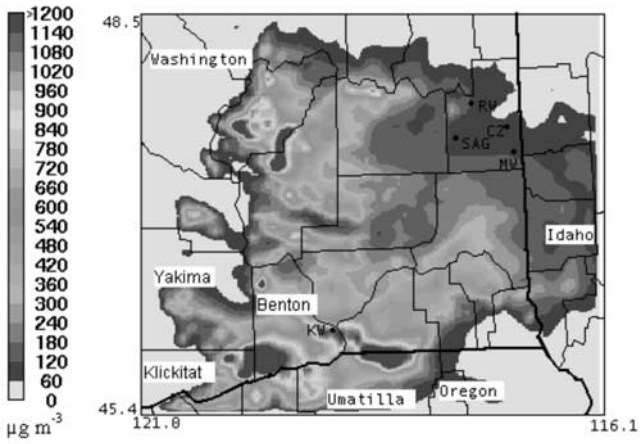

Figure 7. Predicted average 24-hour PM_{10} concentrations, 3 November 1993. See color version of this figure in the HTML.

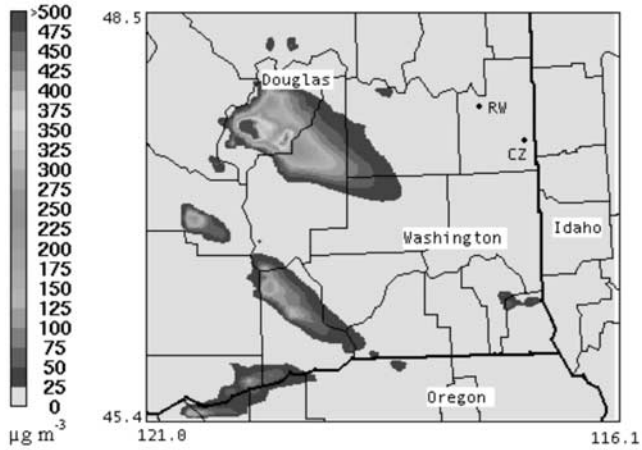

Figure 9. Predicted average 24-hour PM_{10} concentrations, 30 August 1996. See color version of this figure in the HTML.

[32] The statistical tests applied are index of agreement (D), fractional bias (FB) and normalized mean square error (NMSE) [*Elbir*, 2003; *Karppinen et al.*, 2000]. D and NMSE are measures of the correlation of the predicted and measured time series and FB is a measure of agreement of the mean concentrations. Ideally, D should be 100%, and NMSE should be the smallest value possible to reflect smaller variance around the mean value. A large positive value for FB reflects an underprediction whereas a negative value implies that the data has been overpredicted [*Karppinen et al.*, 2000].

[33] The best overall model performance in terms of meteorological predictions was the 23–25 September 1999 event. D for both wind speeds and wind directions were 95% and FB and NMSE were close to 0%. For all the other events, D for wind speeds ranged from 60 to 80% and for wind directions, ranged from 30 to 70%. Wind directions for the 30 August 1996 event were poorly predicted, as reflected in the large FB value (17%). This event also had the largest NMSE value (3%) among all the events and a relatively low D value of 60%.

[34] Table 6 is an overall summary of the six modeled events in this study, tabulated against several factors, including the predicted average 24-hour wind speeds, percentage of cell hours when wind speeds exceeded the predetermined threshold wind speed of 5.5 m s^{-1}, maximum observed PM_{10} concentrations and the ratio of observed to predicted PM_{10} concentrations. The maximum observed PM_{10} concentration highlights the maximum concentration recorded by a sampling station during each dust storm event over the course of 24 or 72 hours. The values in the last column of Table 6 show the average observed to predicted PM_{10} concentration ratios (for all stations) for each event.

[35] The first four events in Table 6 were strong dust storm events with average wind speeds ranging from 6.1 to 7.8 m s^{-1}, corresponding to a significant amount of the cells within the erodible region predicted to have winds sustained above 5.5 m s^{-1} for the 24-hour duration. These strong events were also characterized by high concentrations of PM_{10} observed at the sampling stations. For three of the events presented in Table 6, the ratios of observed to

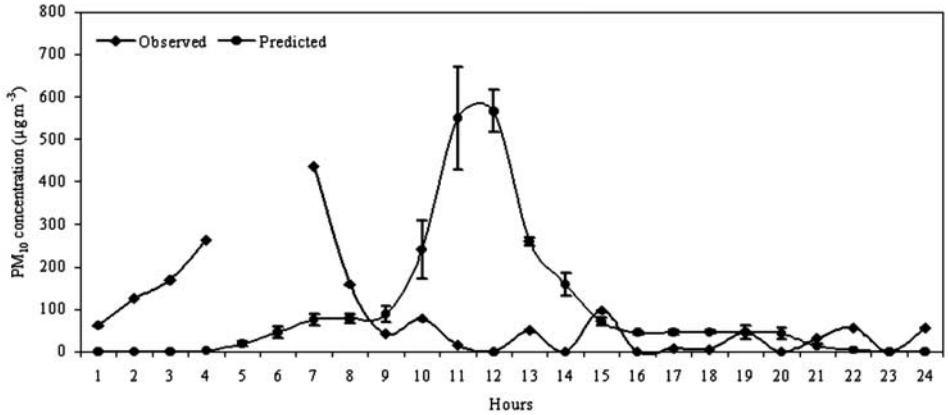

Figure 8. Predicted and measured PM_{10} concentrations at RW, 3 November 1993. See color version of this figure in the HTML.

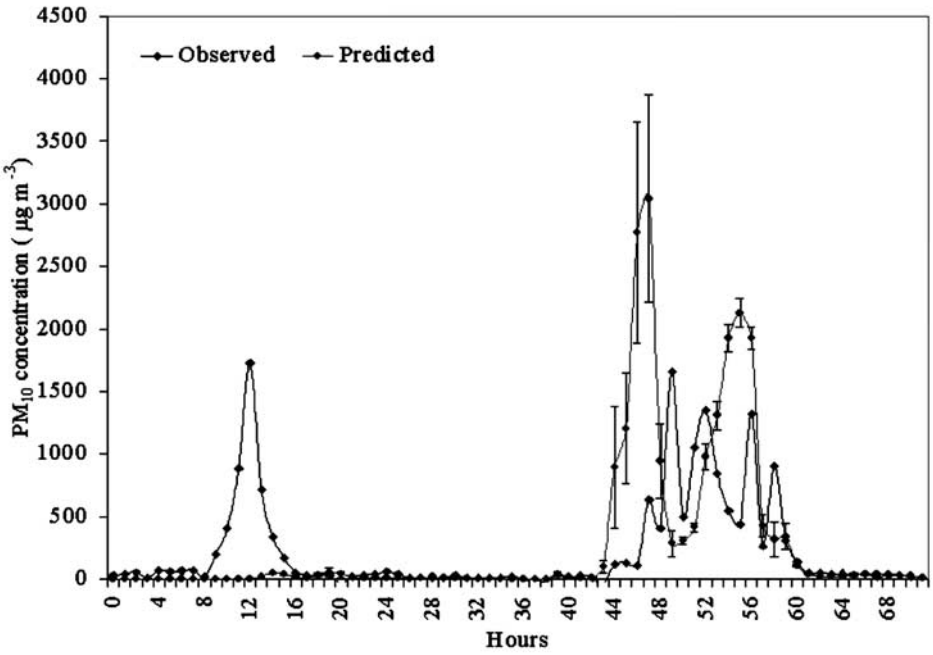

Figure 10. Predicted and measured PM_{10} concentrations at KW, 23–25 September 1999. See color version of this figure in the HTML.

predicted concentrations are less than 2 which is quite good in comparison to the amount of calibration required in previous simulations with this system [*Claiborn et al.*, 1998; *Lee*, 1998]. In the remaining events, the ratios are 3.7, 6.5 and 155, which indicates significant underestimation of the observed PM_{10} levels. Given the fact that the observed and predicted wind speeds are in good agreement, the results for the events suggest either errors in predicting the occurrence of emission, i.e., too high threshold velocity, or error in the plume transport direction, i.e., the plume misses the receptors.

[36] These potential sources of errors were analyzed in the context of the 30 August 1996 event. From the statistical analyses, wind directions for this event were the most

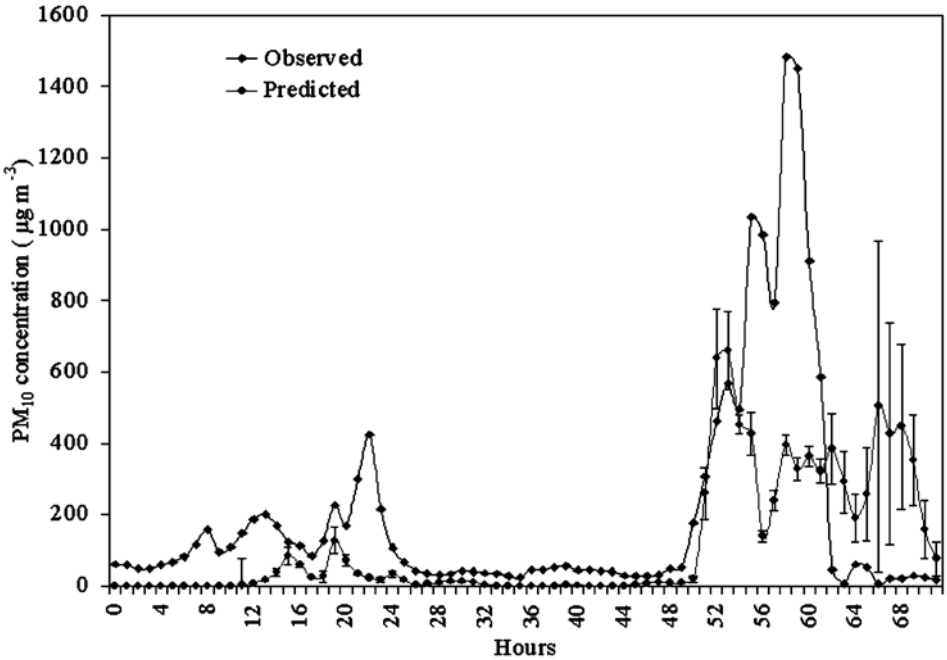

Figure 11. Predicted and measured PM_{10} concentrations at CZ, 23–25 September 1999. See color version of this figure in the HTML.

Table 5. Summary of Meteorological Performance Statistics for Selected Urban Locations for Each Event[a]

	D, %		FB, %		NMSE, %	
Event	WS	WD	WS	WD	WS	WD
23 Nov. 1990	65	70	1.1	5.0	1×10^{-2}	2.5×10^{-1}
21 Oct. 1991	79	40	3.1	9.8	9×10^{-2}	1.0
11 Sept. 1993	81	29	5.7	8.6	3.2×10^{-1}	7.5×10^{-1}
3 Nov. 1993	83	27	12	3.6	1.4	1.3×10^{-1}
30 Aug. 1996	80	60	−8.0	17	6.3×10^{-1}	3.0
23–25 Sept. 1999	99	95	-8.0×10^{-1}	4.3×10^{-1}	6.0×10^{-3}	2.0×10^{-3}

[a]D, index of agreement; FB, fractional bias; NMSE, normalized mean square error; WS, wind speed; and WD, wind direction.

inaccurately represented (FB of 17%) and while correlation between measured and predicted wind directions (D) was not the lowest, it could certainly have compounded the effect of maintaining a nonvarying U_{te} at 5.5 m s^{-1}. *Xuan and Sokolik* [2002] successfully utilized a constant threshold wind speed to identify dust sources in Northern China but studies [*Draxler et al.*, 2001] have shown that parameterizing this variable to roughness parameters to different soil classes would be more representative and future improvements to EMIT-PM should consider this aspect.

[37] In EMIT-PM, U_{te} was determined through visual observations to range from 4.4 to 6.6 m s^{-1} and is linearly parameterized to PM_{10} flux in the emissions algorithm. Decreasing U_{te} to 4.4 m s^{-1} increased PM_{10} concentrations for the 30 August 1996 event by 30–50%. Another important emission variable is WC, and increasing soil dryness (WC values approaching 1 in several land use categories) and, hence, soil erosivity, resulted in a 20–40% increase in PM_{10} emissions, mainly from dry fallow lands. However, even though the overall intensity of the event increased with decreasing U_{te} and increasing WC, the receptors in the 30 August 1996 event were still not significantly impacted by the dust plume because of the predicted wind directions, which were consistently toward the southeast in the modeling domain (Figure 9). The overall results suggest the model performed better at predicting PM_{10} concentrations of large events characterized by average wind speeds exceeding 5.5 m s^{-1} and PM_{10} concentrations exceeding 300 μg m^{-3}. *Draxler et al.* [2001] also observed this trend in their model, which successfully predicted large-scale events (>1000 μg m^{-3}) while overpredicting small-scale events (100 to 200 μg m^{-3}).

[38] Table 7 presents the amount of PM_{10} emitted in the modeling domain as a function of the different land use categories for each event. The 23–25 September 1999 event resulted in the largest PM_{10} emissions (74 Gg), with approximately 95% from DF lands. Among the dust storms that lasted 24 hours, whereas the 23 November 1990 event resulted in the largest PM_{10} emission at 30 Gg, with approximately 61% from DF lands and 37% from IRR lands. These emissions represent a significant loss of fine particles and nutrient content from the agricultural regions in eastern Washington. The 30 August 1996 event had the lowest PM_{10} emission at 2.3 Gg. In general, however, the average loss of PM_{10} soil for a 24-hour dust storm event in eastern Washington (excluding the 30 August 1996 event) was 22 Gg. In terms of contribution toward the global dust loading, an average regional dust storm from eastern Washington represents about 0.5–1% of the global daily average dust flux (based on estimated 1604 Tg yr^{-1} for 0.1–6 μm radius particles, from *Ginoux et al.* [2001]).

[39] Besides improving meteorological predictions and PM_{10} emission parameterizations, it is also important to express soil emissions algorithm in terms of key variables most likely to change as agricultural practices evolve under the stress of adapting to new economic trends and technologies. In eastern Washington, since DF lands are the largest contributors among all the landuse categories to dust emissions and conversion to DC or CRP should reduce the erosivity of the soil, especially during occasions of high wind speeds. However, increasing the surface cover and/or wetness on DF lands may also reduce erosivity potentials by a comparable magnitude. In the Southern High Plains of the United States, which is a source of dust during periods of high-wind events, *Stout and Lee* [2003] documented a decline of 18% in the fraction of potentially erodible cropland between 1982 and 1987. They attributed this decline to the introduction of CRP in 1986, which may have led to a reduction in reported hours of blowing dust from 1985 to 1987. The capability to predict the effects of evolving agricultural practices on dust emission is certainly vital to avoid adverse impacts on regional air quality.

5. Conclusions

[40] The CP^3 windblown dust modeling system with the incorporation of MM5 and MCIP2 was applied to simulate six major dust storm events to predict dust source locations

Table 6. Summary of Modeled Events

Event	24-Hour Average Wind Speeds, m s^{-1}	Percent Cell Hours (Wind Speeds > 5.5 m s^{-1})	Maximum Observed PM_{10}, μg m^{-3}	Observed/Predicted PM_{10} Concentrations
23 Nov. 1990	7.8	86	332	0.7
21 Oct. 1991	6.3	17	1035	6.5
11 Sept. 1993	6.1	46	490	3.7
3 Nov. 1993	7.3	29	1166	1.9
30 Aug. 1996	4.1	14	212	155
23–25 Sept. 1999	5.6	34	1731	1.7

Table 7. Predicted PM_{10} Emissions From Land Use Categories[a]

Event	RL	IRR	DC	DF	CRP
23 Nov. 1990	431	11,202	60	18,739	38
21 Oct. 1991	89	1805	37	7247	10
11 Sept. 1993	140	483	28	13,313	22
3 Nov. 1993	298	7515	99	24,031	46
30 Aug. 1996	12	256	2	2080	2
23–25 Sept. 1999	480	2801	173	70,427	61

[a]PM_{10} emissions are given in Mg. Land use categories are rangeland (RL), irrigated (IRR), dry crop (DC), dry fallow (DF), and conservation resource program (CRP).

in eastern Washington, quantify PM_{10} emissions during a dust storm event and PM_{10} concentrations in downwind urban areas. PM_{10} emissions were estimated on the basis of soil type and land use data common to regions practicing dry land agriculture, with incorporation of other aspects including soil moisture, roughness length and threshold wind velocities. This study employed a more consistent approach to modeling meteorology, which is the main driver to windblown dust events and the subsequent transport and dispersion of the emitted PM_{10}, than our previous modeling studies.

[41] Parameterization of various soil characteristics in the emission model was generally accurate and is reflected in the excellent agreements between predicted and modeled PM_{10} concentrations (less than 2) for three of the dust storm events: 23 November 1990, 3 November 1993 and 23–25 September 1999. The 21 October 1991 and 11 September 1993 events were underpredicted with corresponding observed to predicted PM_{10} concentration ratios of 6.5 and 3.7, respectively. The 30 August 1996 event was poorly represented with a corresponding observed to predicted PM_{10} concentration ratio of 155. Even though these ratios are based on observations from a limited number of sampling stations in Benton and Spokane counties, this range of ratios reflects the inherent complications associated with accurate predictions of plume width and directions, which are correlated to the size of a dust storm event. In terms of fine particle emissions, PM_{10} emissions ranged from an average of 21 Gg for a 24-hour dust storm event to 74 Gg for a 72-hour dust storm event.

[42] The ability to simulate individual dust episodes and identify potential dust regions is an important aspect of regional models. In terms of global dust loading, windblown dust from agricultural regions are potentially important contributions, and results from high-resolution models could be used to complement global-scale models, which generally have horizontal resolutions in the range of 4°–5° and thus are unable to replicate daily and seasonal evolution of dust emissions, transport, deposition and turbidity near dusty regions [*Tegen*, 2003]. Employing even higher horizontal resolutions (e.g., 1 km) may improve subgrid heterogeneities due to wind field variabilites but will require much improved parameterizations of emission factors such as threshold wind speeds, soil surface cover, roughness elements and soil water content. However, higher-resolution models would also aid in improving identification of dust sources and quantifications of fine particles emissions. These aspects should be considered in future studies.

[43] **Acknowledgments.** This work has been supported by the USDA ARS Columbia Plateau (CP^3) PM_{10} project. We would like to thank Joseph Vaughan at WSU and Susan O'Neill, U.S. Forest Service, Seattle, Washington, for their invaluable assistance with this work. We would also like to thank all the members of the CP^3 project for their cooperation.

References

Alfaro, S. C., and L. Gomes (2001), Modelling mineral aerosol production by wind erosion: Emission intensities and aerosol distributions in source areas, *J. Geophys. Res.*, *106*, 18,075–18,084.

Chandler, D. G., K. E. Saxton, J. Kjelgaard, and A. J. Busacca (2002), A technique to measure fine-dust emission potentials during wind erosion, *J. Soil Sci. Soc. Am.*, *66*, 1127–1133.

Claiborn, C., B. Lamb, A. Miller, J. Beseda, B. Clode, J. Vaughan, L. Kang, and C. Newvine (1998), Regional measurements and modeling of windblown agricultural dust: The Columbia Plateau PM_{10} program, *J. Geophys. Res.*, *103*, 19,753–19,767.

Draxler, R. R., D. A. Gillette, J. S. Kirkpatrick, and J. Heller (2001), Estimating PM_{10} air concentrations from dust storms in Iraq, Kuwait and Saudi Arabia, *Atmos. Environ.*, *35*, 4315–4330.

Dudhia, J., D. Gill, Y.-R. Guo, K. Manning, J. Michalakes, A. Bourgeois, W. Wang, and J. Wilson (2001), PSU/NCAR mesoscale modeling system tutorial class notes and user's guide, MM5 Modeling System Version 3, 281 pp., Mesoscale and Microscale Meteorol. Div., Natl. Cent. for Atmos. Res., Colo.

Elbir, T. (2003), Comparison of model predictions with the data of an urban air quality monitoring network in Izmir, Turkey, *Atmos. Environ.*, *37*, 2149–2157.

Fryrear, D. W., J. E. Stout, L. J. Hagen, and E. D. Vories (1991), Wind erosion: Field measurement and analysis, *Trans. ASAE*, *34*, 155–160.

Ginoux, P., M. Chin, I. Tegen, J. M. Prospero, B. Holben, O. Dubovik, and S.-J. Lin (2001), Sources and distributions of dust aerosols simulated with the GOCART model, *J. Geophys. Res.*, *106*, 20,255–20,273.

Gomes, L., J. L. Rajot, S. C. Alfaro, and A. Gaudichet (2003), Validation of a dust production model from measurements performed in semi-arid agricultural areas of Spain and Niger, *Catena*, *52*, 257–271.

Horning, L. B., L. D. Stetler, and K. E. Saxton (1998), Surface residue and soil roughness for wind erosion protection, *Trans. ASAE*, *41*, 1061–1065.

Houser, C. A., and W. G. Nickling (2001), The emission and vertical flux of particulate matter <10 μm from a disturbed clay-crusted surface, *Sedimentology*, *48*, 255–267.

Karppinen, A., J. Kukkonen, T. Elolahde, M. Konttinen, and T. Koskentalo (2000), A modeling system for predicting urban air pollution: Comparisons of model prediction with the data of an urban measurement network in Helsinki, *Atmos. Environ.*, *34*, 3735–3743.

Kim, K. W., Y. J. Kim, and S. J. Oh (2001), Visibility impairment during Yellow Sand periods in the urban atmosphere of Kwangju, Korea, *Atmos. Environ.*, *35*, 5157–5167.

Larney, F. H., M. S. Bullock, S. M. McGinn, and D. W. Fryrear (1995), Quantifying wind erosion on summer fallow in southern Alberta, *J. Soil Water Conserv.*, *50*, 91–95.

Lee, B.-H. (1998), Regional air quality modeling of PM_{10} due to windblown dust on the Columbia Plateau, M.S. thesis, Wash. State Univ., Pullman.

Saxton, K. E. (1995), Wind erosion and its impact on off-site air quality in the Columbia Plateau: An integrated research plan, *Trans. ASAE*, *38*, 1031–1038.

Saxton, K. E., D. Chandler, L. Stetler, B. Lamb, C. Claiborn, and B.-H. Lee (2000), Wind erosion and fugitive dust fluxes on agricultural lands in the Pacific Northwest, *Trans. ASAE*, *43*, 623–630.

Scire, J. S., R. J. Yamartino, G. R. Carmichel, and Y. S. Chang (1989), *CALGRID: A Mesoscale Photochemical Grid Model*, vol. 11, *User*'s *Guide*, 178 pp., State of Calif. Resour. Board, Sacramento.

Scire, J. S., F. R. Robe, M. E. Fernau, and R. J. Yamartino (1999), *A User*'s *Guide for the CALMET Meteorological Mode (Version 5. 0)*, 214 pp., Earth Tech, Inc., Long Beach, Calif.

Stout, J. E. (2001), Dust and environment in the Southern High Plains of North America, *J. Arid Environ.*, *47*, 425–441.

Stout, J. E., and J. A. Lee (2003), Indirect evidence of wind erosion trends on the Southern High Plains of North America, *J. Arid Environ.*, *55*, 43–61.

Tegen, I. (2003), Modeling mineral dust aerosol cycle in the climate system, *Quat. Sci. Rev.*, *22*, 1821–1834.

Tegen, I., and I. Fung (1994), Modeling of mineral dust in the atmosphere: Sources, transport, and optical thickness, *J. Geophys. Res.*, *99*, 22,897–22,914.

Tegen, I., and I. Fung (1995), Contribution to the atmospheric mineral aerosol load from land surface modification, *J. Geophys. Res.*, *100*, 18,707–18,726.

Xuan, J., and I. N. Sokolik (2002), Characterizations of sources and emission rates of mineral dust in Northern China, *Atmos. Environ.*, *36*, 4863–4876.

Yamartino, R. J., J. S. Scire, G. R. Carmichael, and Y. S. Chang (1992), The CALGRID Mesoscale photochemical grid model: I. Model formulation, *Atmos. Environ., Part A*, *26*, 1493–1512.

Yu, S., C. S. Zender, and V. K. Saxena (2001), Direct radiative forcing and atmospheric absorption by boundary layer aerosol in southwestern US: Model estimates on the basis of new observations, *Atmos. Environ.*, *35*, 3967–3977.

D. Chandler, Department of Plants, Soils and Biometeorology, Utah State University, Logan, UT 84322, USA.

C. Claiborn, B. Lamb, T. Strand, and I. Sundram, Laboratory for Atmospheric Research, Department of Civil and Environmental Engineering, Washington State University, Pullman, WA 99164, USA. (irra_t-mohanasu@wsu.edu)

K. Saxton, USDA-ARS, Washington State University, L. J. Smith Hall, Pullman, WA 99165, USA.